Short Papers

Analysis of Complementary Unilateral Slot and Strip Resonators Printed on Anisotropic Substrates

Yinchao Chen and Benjamin Beker

***Abstract*—A systematic method, based on the two-dimensional spectral domain method, for analyzing complementary unilateral slot and strip resonators is presented. The resonators are printed on anisotropic substrates with tensor permittivity and permeability, including the off-diagonal terms and ferrite properties. Numerical data are presented to illustrate the response of resonators to changes in material properties of the substrate.**

I. Introduction

Microwave resonators are extensively used as building blocks in fin-line filter, oscillator, and mixer design [1], [2]. Many techniques have been applied to analyze a variety of microwave resonators using approximate and full wave methods [2]–[6]. Increasing use of anisotropic materials in millimeter-wave integrated circuit applications [7] and high-speed digital circuits [8] requires thorough examination to determine the influence of such materials on the performance of the resonator.

In this paper, the two-dimensional (2-D) spectral domain approach is used to investigate the properties of complementary microwave resonators, i.e., suspended unilateral slot and strip resonators. Unlike the earlier work [1]–[6], resonators considered herein are printed on anisotropic substrates characterized by both permittivity and permeability tensors, including off-diagonal terms. The boundary value problem is formulated in the Fourier-transformed domain, which leads to impedance and admittance Green's functions for strip and slot structures, respectively. The resonant frequencies are computed as functions of changing tensor elements of the substrate.

II. Summary of the Formulation

Consider a pair of complementary structures, i.e., the suspended unilateral slot and strip resonators, as well as their coordinate system, shown in Fig. 1. According to [9], to account for the off-diagonal terms of the permittivity and the Hermitan nature of permeability, the two medium tensors will be given as

$$\kappa_0[\kappa_r] = \kappa_0 \begin{bmatrix} \kappa_{xx} & 0 & \kappa_{xz} \\ 0 & \kappa_{yy} & 0 \\ \kappa_{zx} & 0 & \kappa_{zz} \end{bmatrix} \qquad (\kappa = \varepsilon \text{ or } \mu). \tag{1a,b}$$

For the resonator boundary value problem depicted in Fig. 1, a 2-D Fourier transform with respect to x and z coordinates is used

Manuscript received May 12, 1994; revised December 14, 1994. This work was supported by the U.S. Army Research Office Grant DAALO3-92-G-0275.

The authors are with the Department of Electrical and Computer Engineering, University of South Carolina, Columbia, SC 29208 USA.

IEEE Log Number 9412059.

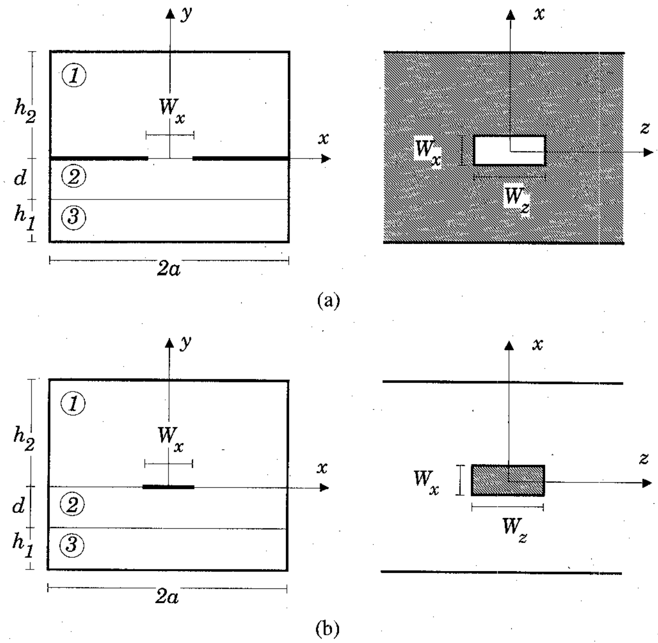

Fig. 1. Cross-sectional and top views of the unilateral slot (a) and strip (b) resonators.

along with differential matrix operators [10] to obtain the following Green's functions

$$\begin{bmatrix} \begin{pmatrix} \tilde{Z}_{zz}(\alpha,\beta) \\ \tilde{Y}_{zz}(\alpha,\beta) \end{pmatrix} & \begin{pmatrix} \tilde{Z}_{zx}(\alpha,\beta) \\ \tilde{Y}_{zx}(\alpha,\beta) \end{pmatrix} \\ \begin{pmatrix} \tilde{Z}_{xz}(\alpha,\beta) \\ \tilde{Y}_{xz}(\alpha,\beta) \end{pmatrix} & \begin{pmatrix} \tilde{Z}_{xx}(\alpha,\beta) \\ \tilde{Y}_{xx}(\alpha,\beta) \end{pmatrix} \end{bmatrix} \begin{bmatrix} \begin{pmatrix} \tilde{J}_z(\alpha,\beta) \\ \tilde{E}_z(\alpha,\beta) \end{pmatrix} \\ \begin{pmatrix} \tilde{J}_x(\alpha,\beta) \\ \tilde{E}_x(\alpha,\beta) \end{pmatrix} \end{bmatrix} = \begin{bmatrix} \begin{pmatrix} \tilde{E}_z(\alpha,\beta) \\ \tilde{J}_z(\alpha,\beta) \end{pmatrix} \\ \begin{pmatrix} \tilde{E}_x(\alpha,\beta) \\ \tilde{J}_x(\alpha,\beta) \end{pmatrix} \end{bmatrix}. \tag{2a,b}$$

In the above expressions, the impedance Green's function $[Z]$ and admittance Green's function $[Y]$ correspond to the suspended unilateral strip and slot resonators, respectively. The explicit forms of the Green's function elements are given in the Appendix.

Accurate and efficient calculations of the resonant frequencies are greatly dependent on the choice of basis functions. Similar to those in [11], the basis functions, satisfying edge conditions of the slot and strip on the $y = 0$ plane, are chosen to be

$$\begin{pmatrix} E_x \\ J_z \end{pmatrix} = \frac{1}{\sqrt{1-(2x/W_x)^2}} \frac{\cos\left(\frac{\pi z}{W_z}\right)}{\sqrt{1-(2z/W_z)^2}} U_x U_z \tag{3a,b}$$

$$\begin{pmatrix} E_z \\ J_x \end{pmatrix} = \frac{\sin\left(\frac{2\pi x}{W_x}\right)}{\sqrt{1-(2x/W_x)^2}} \frac{\sin\left(\frac{\pi z}{W_z}\right)}{\sqrt{1-(2z/W_z)^2}} U_x U_z \tag{3c,d}$$

where *Heaviside* unit step functions

$$U_i = U\left(i + \frac{W_i}{2}\right) - U\left(i - \frac{W_i}{2}\right) \quad (i = x, z) \tag{4}$$

are used to define the basis functions over the slot or strip only.

TABLE I
COMPARISON DATA FOR SUSPENDED SLOT AND STRIP RESONATORS

W_z (mm)	f_r slot	f_r from [1]	W_z (mm)	f_r strip	f_r from [2]
3.25	34.50	34.7	8	16.27	15.8
3.75	32.54	32.6	10	13.30	12.7
4.25	30.27	30.4	12	11.25	10.9
$2a = 3.556$	$h_1 = 2.8$	$d = 0.127$	$2a = 10.0$	$h_1 = 0.125$	$d = 0.127$
$\varepsilon_{r2} = 2.2$	$h_2 = 4.185$	$W_x = 0.3556$	$\varepsilon_{r2} = 2.2$	$h_2 = 1.298$	$W_x = 0.5$

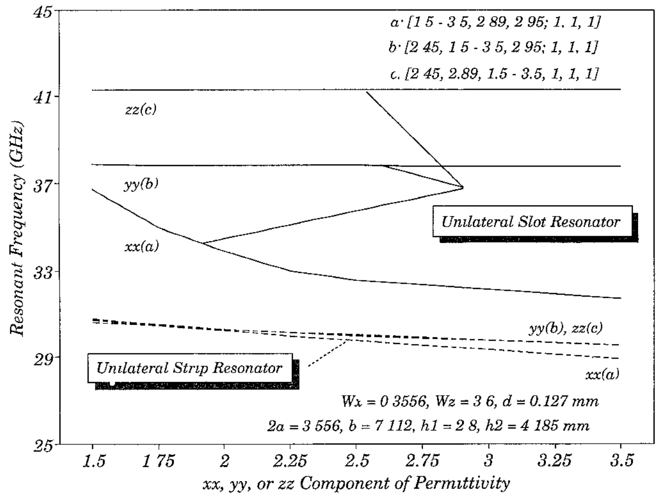

Fig. 2. f_r for slot and strip resonators as a function of the permittivity tensor elements (regions 1 and 2 are air).

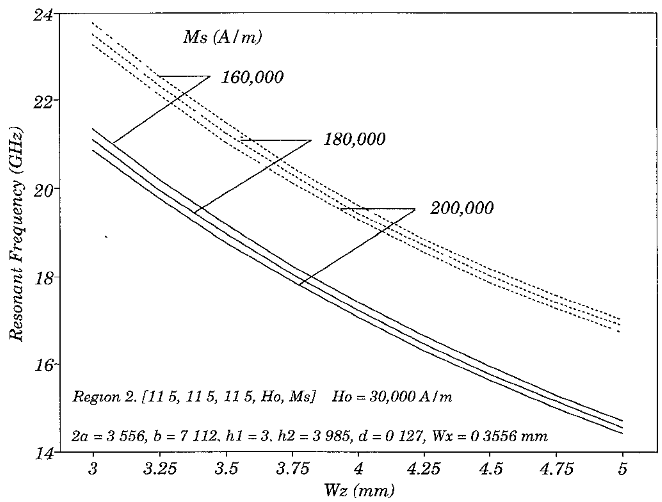

Fig. 3. f_r for slot (dashed lines) and strip (solid lines) resonators as a function of M_s (regions 1 and 3 are air).

Finally, Galerkin's method is implemented to set up a system of linear equations from which the resonant frequencies, f_r, of the structure can be determined by setting the system determinant to zero and searching for the roots.

III. NUMERICAL RESULTS

The SDA for the slot and strip resonators was validated against previously published data for both structures. Numerical results for suspended unilateral slots and strips printed on isotropic substrates were compared to data available in [1], [2], with selected data points listed in the following table. For the computations, the permittivity of regions 1 and 3 was assumed to be air, with all other dimensions and the dielectric constant of the substrate listed in the table. As can be seen from the results of Table I, very good agreement was obtained for both structures, validating the numerical solution to the three-region boundary value problem.

The effects of varying element values of the permittivity tensors were investigated for both resonators and the results are shown in Fig. 2. It was found that the resonant frequency of the slot resonator is more sensitive to changes in ε_{xx}, than to changes in any other element. The same is also true for the strip resonator. However, the overall change in f_r is significantly lower than for the slot.

Finally, Fig. 3 summarizes the effects of W_z on f_r when the resonators are printed on the substrate that has the properties of the Ferrite. The magnetic tensor has a Hermitian form and is a function of H_0 and M_s; namely, the magnitude of biasing field and magnetization. For each structure, M_s is allowed to vary from 160–200 (kA/m). The resonant frequencies are seen to decrease with increasing resonant length from 24–16 GHz and from 22–14 GHz for slot and strip resonators, respectively. The effect of magnetization on both structures is the same, reducing f_r for increasing values of M_s.

IV. CONCLUSION

Resonant properties of complementary unilateral slot and strip resonators printed on anisotropic substrates were investigated using the spectral domain approach. The Green's functions were derived in the Fourier-transform domain and Galerkin's method was used for finding the resonant frequencies. Effects of substrate anisotropy on the resonant frequencies were examined.

APPENDIX

In (2), where $[Y] = [Z]^{-1}$, the elements of impedance Green's functions can be written as

$$\tilde{Z}_{zz} = \frac{y_b r_z - y_a s_z}{x_a y_b - x_b y_a} \qquad \tilde{Z}_{zx} = \frac{x_b r_z - x_a s_z}{x_a y_b - x_b y_a} \qquad \text{(A-1a,b)}$$

$$\tilde{Z}_{xz} = \frac{y_b r_x - y_a s_x}{x_a y_b - x_b y_a} \qquad \tilde{Z}_{xx} = \frac{x_b r_x - x_a s_x}{x_a y_b - x_b y_a} \qquad \text{(A-1c,d)}$$

where

$$\begin{bmatrix} r_z \\ s_z \end{bmatrix} = 1 + \frac{1}{\Delta t} \begin{bmatrix} ct_2^a (s_{11} t_{22} - s_{21} t_{12}) \\ \frac{c_2^a}{s_2^b} (s_{12} t_{22} - s_{22} t_{12}) \end{bmatrix} + \frac{1}{\Delta t} \begin{bmatrix} \frac{c_2^b}{s_2^a} (s_{21} t_{11} - s_{11} t_{21}) \\ ct_2^b (s_{22} t_{11} - s_{12} t_{21}) \end{bmatrix} \qquad \text{(A-2a,b)}$$

$$\begin{bmatrix} r_x \\ s_x \end{bmatrix} = \begin{bmatrix} \eta_a \\ \eta_b \end{bmatrix} + \frac{1}{\Delta t} \begin{bmatrix} \eta_a ct_2^a (s_{11} t_{22} - s_{21} t_{12}) \\ \eta_a \frac{c_2^a}{s_2^b} (s_{12} t_{22} - s_{22} t_{12}) \end{bmatrix} + \frac{1}{\Delta t} \begin{bmatrix} \eta_b \frac{c_2^b}{s_2^a} (s_{21} t_{11} - s_{11} t_{21}) \\ \eta_b ct_2^b (s_{22} t_{11} - s_{12} t_{21}) \end{bmatrix} \qquad \text{(A-2c,d)}$$

$$\begin{bmatrix} x_a \\ x_b \end{bmatrix} = \begin{bmatrix} u_1 \\ u_3 \end{bmatrix} + \frac{u_2}{\Delta t}\begin{bmatrix} ct_2^a(s_{11}t_{22} - s_{21}t_{12}) \\ \frac{c_2^a}{s_2^b}(s_{12}t_{22} - s_{22}t_{12}) \end{bmatrix} + \frac{u_4}{\Delta t}\begin{bmatrix} \frac{c_2^b}{s_2^a}(s_{21}t_{11} - s_{11}t_{21}) \\ ct_2^b(s_{22}t_{11} - s_{12}t_{21}) \end{bmatrix} \quad \text{(A-3a,b)}$$

$$\begin{bmatrix} y_a \\ y_b \end{bmatrix} = \begin{bmatrix} v_1 \\ v_3 \end{bmatrix} + \frac{v_2}{\Delta t}\begin{bmatrix} ct_2^a(s_{11}t_{22} - s_{21}t_{12}) \\ \frac{c_2^a}{s_2^b}(s_{12}t_{22} - s_{22}t_{12}) \end{bmatrix} + \frac{v_4}{\Delta t}\begin{bmatrix} \frac{c_2^b}{s_2^a}(s_{21}t_{11} - s_{11}t_{21}) \\ ct_2^b(s_{22}t_{11} - s_{12}t_{21}) \end{bmatrix} \quad \text{(A-3c,d)}$$

$$\begin{bmatrix} s_{11} \\ s_{12} \end{bmatrix} = \frac{\left(h_{11}\begin{pmatrix} \eta_a \\ \eta_b \end{pmatrix} + h_{12}\right)}{z_0\mu_d G}\begin{bmatrix} \gamma_a \\ \gamma_b \end{bmatrix}$$

$$\begin{bmatrix} s_{21} \\ s_{12} \end{bmatrix} = \frac{\left(h_{21}\begin{pmatrix} \eta_a \\ \eta_b \end{pmatrix} + h_{22}\right)}{z_0\mu_d G}\begin{bmatrix} \gamma_a \\ \gamma_b \end{bmatrix} \quad \text{(A-4a,b,c,d)}$$

$$\begin{bmatrix} t_{11} \\ t_{12} \end{bmatrix} = \left\{ \frac{-\beta y_0}{(\alpha^2+\beta^2)\gamma_3}\left(\alpha\begin{bmatrix} \eta_a \\ \eta_b \end{bmatrix} + \beta\right) + \frac{\alpha\gamma_3}{(\alpha^2+\beta^2)z_0}\left(\beta\begin{bmatrix} \eta_a \\ \eta_b \end{bmatrix} - \alpha\right)\right\} ct_3 \quad \text{(A-5a,b)}$$

$$\begin{bmatrix} t_{21} \\ t_{22} \end{bmatrix} = \left\{ \frac{\alpha y_0}{(\alpha^2+\beta^2)\gamma_3}\left(\alpha\begin{bmatrix} \eta_a \\ \eta_b \end{bmatrix} + \beta\right) + \frac{\beta\gamma_3}{(\alpha^2+\beta^2)z_0}\left(\beta\begin{bmatrix} \eta_a \\ \eta_b \end{bmatrix} - \alpha\right)\right\} ct_3 \quad \text{(A-5c,d)}$$

with

$$\begin{bmatrix} u_1 \\ u_2 \end{bmatrix} = \frac{\gamma_a(h_{11}\eta_a + h_{12})}{z_0\mu_d G}\begin{bmatrix} ct_2^a \\ th_2^a \end{bmatrix} - \frac{\beta ct_1 y_0(\alpha\eta_a + \beta)}{\gamma_1(\alpha^2+\beta^2)} + \frac{\alpha\gamma_1 ct_1(\beta\eta_a - \alpha)}{z_0(\alpha^2+\beta^2)} \quad \text{(A-6a,b)}$$

$$\begin{bmatrix} u_3 \\ u_4 \end{bmatrix} = \frac{\gamma_b(h_{11}\eta_b + h_{12})}{z_0\mu_d G}\begin{bmatrix} ct_2^b \\ th_2^b \end{bmatrix} - \frac{\beta ct_1 y_0(\alpha\eta_b + \beta)}{\gamma_1(\alpha^2+\beta^2)} + \frac{\alpha\gamma_1 ct_1(\beta\eta_b - \alpha)}{z_0(\alpha^2+\beta^2)} \quad \text{(A-6c,d)}$$

$$\begin{bmatrix} v_1 \\ v_2 \end{bmatrix} = \frac{\gamma_a(h_{21}\eta_a + h_{22})}{z_0\mu_d G}\begin{bmatrix} ct_2^a \\ th_2^a \end{bmatrix} + \frac{\alpha ct_1 y_0(\alpha\eta_a + \beta)}{\gamma_1(\alpha^2+\beta^2)} + \frac{\beta\gamma_1 ct_1(\beta\eta_a - \alpha)}{z_0(\alpha^2+\beta^2)} \quad \text{(A-7a,b)}$$

$$\begin{bmatrix} v_3 \\ v_2 \end{bmatrix} = \frac{\gamma_b(h_{21}\eta_b + h_{22})}{z_0\mu_d G}\begin{bmatrix} ct_2^b \\ th_2^b \end{bmatrix} + \frac{\alpha ct_1 y_0(\alpha\eta_b + \beta)}{\gamma_1(\alpha^2+\beta^2)} + \frac{\beta\gamma_1 ct_1(\beta\eta_b - \alpha)}{z_0(\alpha^2+\beta^2)}, \quad \text{(A-7c,d)}$$

where $z_0 = j\omega\mu_0$, $\mu_d = \mu_{xx}\mu_{zz} - \mu_{xz}\mu_{zx}$, and

$$G = \alpha^2\mu_{xx} + \beta^2\mu_{zz} + \alpha\beta(\mu_{xz} + \mu_{zx}) - k_0^2\varepsilon_{yy}\mu_d. \quad \text{(A-7e)}$$

Variables γ_1, $\gamma_{a,b}$, γ_3 are roots of characteristic equations in regions 1, 2, and 3, respectively. The remaining constants appearing in the above equations are given as

$$z_0 = j\omega\mu_0 \qquad y_0 = j\omega\varepsilon_0 \quad \text{(A-8a,b)}$$

$$s_2^{a,b} = \sinh\gamma_{a,b}d \qquad c_2^{a,b} = \cosh\gamma_{a,b}d \quad \text{(A-9a,b)}$$

$$ct_2^{a,b} = \coth\gamma_{a,b}d \qquad th_2^{a,b} = \tanh\gamma_{a,b}d \quad \text{(A-9c,d)}$$

$$ct_1 = \coth\gamma_1 h_2 \qquad ct_3 = \coth\gamma_3 h_1 \quad \text{(A-10a,b)}$$

where ω is the angular frequency.

References

[1] B. Bhat and S. K. Koul, *Analysis, Design and Application of Fin Lines.* Norwood, MA: Artech House, 1987.

[2] S. K. Koul and R. Khanna, "Broadside-coupled rectangular resonators in suspended stripline with single and double dielectrics," *IEE Proc.*, Pt. H, vol. 137, no. 6, pp. 411–414, Dec. 1990.

[3] T. Itoh, "Analysis of microstrip resonators," *IEEE Trans. Microwave Theory Tech.*, vol. MTT-22, no. 11, pp. 946–952, Nov. 1974.

[4] S. Mao, S. Jones, and G. D. Vendilin, "Millimeter-wave integrated circuits," *IEEE Trans. Microwave Theory Tech.*, vol. MTT-16, no. 7, pp. 455–461, July 1968.

[5] T. Uwano, "A small dielectric TEM mode resonator with crossing slot and its application to a cellular radio VCO," *IEEE Trans. Microwave Theory Tech.*, vol. MTT-22, no. 11, pp. 946–952, Nov. 1974.

[6] A. K. Agrawal and B. Bhat, "Characteristics of coupled rectangular slot resonators in fin-line configurations," *Int. J. Electron.*, vol. 58, no. 5, pp. 781–792, 1985.

[7] N. G. Alexopoulos, "Integrated structures on anisotropic substrates," *IEEE Trans. Microwave Theory Tech.*, vol. MTT-33, no. 10, pp. 847–881, Oct. 1985.

[8] A. Deutsch *et al.*, "Dielectric anisotropy of BPDA-PDA polymide and its effect on electrical characteristics of interconnects," in *Proc. 2nd Meet. Elect. Performance Electron., Packaging*, Oct. 1993, pp. 152–154.

[9] Y. Chen and B. Beker, "Spectral-domain analysis of open and shielded slotlines printed on various anisotropic substrates," *IEEE Trans. Microwave Theory Tech.*, vol. MTT-41, no. 11, pp. 1872–1877, Nov. 1993.

[10] Y. Chen and B. Beker, "Dispersion characteristics of open and shielded microstrip lines under a combined principal axes rotation of electrically and magnetically anisotropic substrates," *IEEE Trans. Microwave Theory Tech.*, vol. 41, no. 4, pp. 673–679, Apr. 1993.

[11] T. Itoh and W. Menzel, "A full-wave analysis method for open microstrip structures," *IEEE Trans. Antennas and Propagat.*, vol. AP-29, pp. 63–68, 1981.

Characterization of Cylindrical Microstriplines Mounted Inside a Ground Cylindrical Surface

Ruenn-Bo Tsai and Kin-Lu Wong

***Abstract*—A full-wave analysis for the frequency-dependent characteristics of a cylindrical microstripline mounted inside a ground cylindrical surface is presented. Numerical results of the effective dielectric constant and characteristic impedance for various microstripline parameters are calculated and analyzed. Strong dispersive behavior is observed for such cylindrical microstriplines.**

I. Introduction

For many practical applications, microstrip antennas need to be conformed to curved surfaces. This also makes necessary the design of conformal microstrip circuits that form the excitation network of the antenna. This paper presents the study of a microstripline printed on the inner surface of a cylindrical substrate that is enclosed by a conducting ground cylinder. This kind of cylindrical microstripline can find applications in feeding a slot-coupled cylindrical microstrip antenna [1]. In this case, the energy can be coupled from the microstripline to the antenna through a coupling slot in the cylindrical

Manuscript received August 16, 1994; revised December 19, 1994. This work was supported by the National Science Council of the Republic of China Grant NSC83-0404-E-110-017.

The authors are with the Department of Electrical Engineering, National Sun Yat-Sen University, Kaohsiung, Taiwan 804, R.O.C.

IEEE Log Number 9412031.